



D3.5 Primary Production Product Documentation



This project has received funding from the European Union's Horizon 2020 research and innovation programme under grant agreement No 776348.

Project no. 776348
Project acronym: CoastObs
Project title: Commercial service platform for user-relevant coastal water monitoring services based on Earth Observation
Instrument: H2020-EO-2017
Start date of project: 01.11.2017
Duration: 36 months
Deliverable title: D3.5 Primary Production Product Documentation
Due date of deliverable: Month 19
Organisation name of lead contractor for this deliverable: USTIR

Author list:

Name	Organisation
Caitlin Riddick	University of Stirling
Evangelos Spyrakos	University of Stirling
Peter Hunter	University of Stirling
Andrew Tyler	University of Stirling
Kathrin Poser	Water Insight
Steef Peters	Water Insight

Dissemination level

PU	Public	X
CO	Confidential, restricted under conditions set out in Model Grant Agreement	
CI	Classified, information as referred to in Commission Decision 2001/844/EC	

History			
Version	Date	Reason	Revised by
01	24/05/2019	Initial Draft for review	Caitlin Riddick (USTIR)
02	27/05/2019	Internal Review	Kathrin Poser (WI)
03	30/05/2019	Revised Draft for submission	Caitlin Riddick (USTIR)

Please cite as:

Riddick, C.A.L., Spyrakos, E.S., Hunter, P.D., Tyler, A.N., Poser, K., Peters, S. (2019). D3.5 Primary Production Product Documentation. CoastObs Project.

CoastObs Project

CoastObs is an EU H2020 funded project that aims at using satellite remote sensing to monitor coastal water environments and to develop a user-relevant platform that can offer validated products to users including monitoring of seagrass and macroalgae, phytoplankton size classes, primary production, and harmful algae as well as higher level products such as indicators and integration with predictive models.



phytoplankton



seagrass



harmful algal blooms



primary production

To fulfil this mission, we are in dialogue with users from various sectors including dredging companies, aquaculture businesses, national monitoring institutes, among others, in order to create tailored products at highly reduced costs per user that stick to their requirements.

With the synergistic use of Sentinel-3 and Sentinel-2, CoastObs aims at contributing to the sustainability of the Copernicus program and assisting in implementing and further fine-tuning of European Water Quality related directive.

Partnership



Water Insight BV. (WI)



UNIVERSITY OF
STIRLING

The University of Stirling (USTIR)



Consiglio Nazionale
delle Ricerche

Consiglio Nazionale Delle Ricerche (CNR)



UNIVERSITÉ DE NANTES

Universite de Nantes (UN)



UNIVERSITY
OF APPLIED SCIENCES

HZ University of Applied Sciences (HZ)



UNIVERSIDADE
DE VIGO

Universidad de Vigo (UVIGO)



Bio-Littoral (BL)



GEONARDO
STATE-OF-THE-ART AND BEYOND

Geonardo Environmental Technologies Ltd. (GEO)

TABLE OF CONTENTS

1	Summary.....	7
2	Introduction.....	8
3	Primary Production models.....	9
3.1.1	Empirical models	9
3.1.2	Vertically Generalised Production Model (VGPM).....	9
3.1.3	Wavelength Resolved Models	9
3.1.4	Carbon-based models.....	10
3.1.5	Phytoplankton absorption models	10
4	Initial retuning and validation	11
4.1	Historic dataset.....	11
4.1.1	Methods	11
4.1.2	Performance of <i>in situ</i> empirical model	13
4.1.3	Performance of <i>in situ</i> VGPM	15
4.1.4	Performance of satellite model.....	17
4.2	2018-2019 dataset.....	26
4.2.1	Methods	28
5	Conclusions and future work.....	29
6	References.....	30

FIGURES

Figure 1. Map of Historic PP measurement stations in the Venice Lagoon and Adriatic Sea.	12
Figure 2. Empirical relationship between PP and Chl-a for Venice Lagoon and the Adriatic Sea.	13
Figure 3. In situ validation results for empirical model (as in Behrenfeld et al. 1998)	14
Figure 4. In situ validation results for site-specific empirical models.	14
Figure 5. Validation of (a) VGPM, (b) mVGPM and (c) m2VGPM with in situ data and associated errors.	17
Figure 6. Validation of MERIS L2 algal_2 Chl-a product for Venice Lagoon and the Adriatic Sea.....	18
Figure 7. Validation plot and errors for PP derived from MERIS algal_2 Chl-a using site-specific empirical models.	19
Figure 8. Site specific derived relationship for Zeu as a function of Kd(490) MERIS L2 product in the (a) Adriatic Sea and (b) Venice Lagoon.	21
Figure 9. AATSR L2 gridded sea surface temperature (SST) as a function of in situ SST (°C).	22
Figure 10. GHRSSST as a function of in situ sea surface temperature (°C) for 7 stations in the Eems Estuary, Netherlands (Water Insight, Unpublished data).	23
Figure 11. Validation plot of MERIS L2 surface photosynthetically available radiation (PAR) as a function of in situ surface PAR.	23
Figure 12. MERIS derived Euphotic depth (Zeu) as a function of in situ Zeu.	24
Figure 13. Validation plot and errors for PP _{eu} derived from MERIS and AATSR for the Adriatic Sea...	25
Figure 14. PP derived from MERIS (m2VGPM model; 2005-07-14)	26
Figure 15. The Chelsea Act2 set up for laboratory based simulated in situ measurements by fast repetition rate fluorometry (FRRf).	27

TABLES

Table 1 – Summary of field campaigns completed and planned in support of PP product validation (2018-2019)	27
--	----

1 Summary

Approximately 50% of global net primary production (PP) is attributed to ocean phytoplankton (Field et al., 1998), and this contribution is likely to be even greater in coastal waters. Marine PP is also fundamental to food web dynamics, biogeochemical cycles and marine fisheries (Chassot et al., 2010; Passow and Carlson, 2012). Earth observation (EO) can be a useful tool for monitoring PP in coastal waters, as is of particular interest to CoastObs users (e.g. environmental managers and aquaculture producers). However most satellite derived PP models have been developed and validated using data from open oceans. Therefore, as part of CoastObs we aim to test the published PP models for ocean waters and retune them for coastal waters, in particular for the Venice Lagoon and the Adriatic Sea (Italy), Galician coastal waters (Spain), and the Wadden Sea and Eastern Scheldt (Netherlands).

Therefore, this deliverable outlines the CoastObs PP product documentation, including a description of the methods to be used for the CoastObs PP product. This includes analysis using models retuned using a historic PP dataset for the Venice Lagoon and Adriatic Sea (Italy), then validated using coincident MERIS and AATSR data. In future, the models will be adapted to Sentinel-3 (OLCI and SLSTR) through refined parameterisations and re-tuning. The Sentinel-3 PP model re-tuning and validation results will be presented in the forthcoming Validation Report (D3.8).

2 Introduction

The uptake, transformation and respiration of C by phytoplankton contributes significantly to carbon transfer across the air-water interface. In fact, approximately 50% of global net primary production (PP) is attributed to ocean phytoplankton (Field et al., 1998), and this contribution is likely to be even greater in coastal waters. Phytoplankton PP effectively acts as a “biological pump” that removes carbon from the surface ocean, playing a major role in both regional and global carbon (C) cycling in ocean waters (Passow and Carlson, 2012). Marine PP is also fundamental to food web dynamics, biogeochemical cycles and marine fisheries (Chassot et al., 2010; Passow and Carlson, 2012).

PP is defined as the amount of carbon (or organic material) fixed per area over time (Cloern et al., 2014). The rate of phytoplankton PP is primarily a function of the incident irradiance, light absorption efficiency and the quantum efficiency of carbon fixation and thus has strong dependency on the inherent optical properties (IOPs) of the water column, phytoplankton composition, size structure and photophysiology, and local environmental factors such as water temperature, nutrient availability and vertical mixing.

Earth Observation (EO) can be a useful tool for monitoring PP, and there are several published models for the estimation of PP from satellite-derived data. These have been widely tested and validated in open oceans (Smyth et al. 2005), shelf seas (Tilstone et al. 2005) and coastal waters (Barnes et al. 2014), and range from simple empirical approaches that model PP as a function of the near surface Chl-*a* (e.g. Behrenfeld et al. 1998), depth-integrated models that account for variability in chlorophyll-specific assimilation efficiency for carbon fixation (e.g. Vertically Generalized Production Model (VGPM); Behrenfeld and Falkowski, 1997) and in some cases its dependency on temperature (e.g. Eppley et al. 1972), to more complex models that estimate PP as a function of wavelength (Wavelength Resolved Model (WRM); Morel, 1991). These models typically output an estimate of the daily phytoplankton carbon fixation within the euphotic zone per unit of water surface area (in mg C m⁻² day⁻¹). Most algorithms model PP as a function of the Chl-*a*, however more recent approaches based on phytoplankton absorption (Barnes et al. 2014) or phytoplankton carbon (Behrenfeld et al. 2005; Westberry et al. 2008) have been developed to reduce model uncertainties due to variability in chlorophyll-specific rates of primary production.

Most PP models have been almost exclusively been developed and validated using data from marine waters. As such, their potential applicability to complex coastal waters has not been as widely explored. Therefore, as part of CoastObs we aim to test the published PP models for ocean waters and retune them for coastal waters, in particular for the Venice Lagoon and the Adriatic Sea (Italy), Galician coastal waters (Spain), and the Wadden Sea and Eastern Scheldt (Netherlands). This will include analysis using models calibrated with historic PP data for the Venice Lagoon and Adriatic Sea, then tested and validated using coincident MERIS and AATSR

data. In future, the models will be adapted to Sentinel-3 (OLCI and SLSTR) through refined parameterisations and calibrations.

Therefore, this deliverable outlines the product documentation, including a description of the methods to be used for the CoastObs PP product. Validation results will be presented in **D3.8** (Validation Report).

3 Primary Production models

3.1.1 Empirical models

Empirical models derive PP as a function of the near surface chlorophyll-*a* (Chl-*a*). For example, Eppley et al. (1985) used a simple regression between $\log^{14}\text{C}$ uptake and \log Chl-*a* concentration and found good correlation over a broad range of waters. Behrenfeld et al. (1998) derived the following empirical model, estimating \log PP as a function of \log Chl-*a*:

$$\log_{10}PP = 0.559 * \log_{10}[Chl - a] + 2.793 \quad (1)$$

3.1.2 Vertically Generalised Production Model (VGPM)

Depth-integrated models for PP account for variability in chlorophyll-specific assimilation efficiency for carbon fixation (e.g. Vertically Generalized Production Model (VGPM); Behrenfeld and Falkowski, 1997) and in some cases its dependency on temperature (e.g. Eppley et al. 1972). The VGPM estimates depth integrated primary production (PP_{eu}) from surface chlorophyll-*a* ($Chl-a_s$) using a temperature-dependent description of chlorophyll-specific photosynthetic efficiency ($P^{B_{obt}}$), surface irradiance (E_0), euphotic depth (Z_{eu}) and daily photoperiod (D_{irr}). This model is presented below and described in further detail in Section 4.1.1:

$$PP_{eu} = 0.66125 * (P^{B_{opt}}) * (E_0 / (E_0 + 4.1)) * Z_{eu} * Chl - a_s * D_{irr} \quad (2)$$

3.1.3 Wavelength Resolved Models

Wavelength resolved models (WRM) estimate PP as a function of wavelength (Morel, 1991; Smyth et al., 2005). The daily realised column production (P) is represented as a function of Chlorophyll (Chl), Photosynthetically Available Radiation (PAR), the Chl specific absorption ($a^*(\lambda)$) cross section pertinent to the spectral light field composition, and the net growth rate (ϕ_{μ} , $\text{mol C} (\text{mol quanta})^{-1}$). This function is triple integrated over the euphotic zone depth (Z_{eu} , 1% light level) at each depth (Z), day length (L , seconds) and the spectral light field (as a function of depth, Z) between 400 (λ_1) and 700 (λ_2) nm. This can be expressed as:

$$P = 12 \int_0^L \int_0^D \int_{\lambda_2}^{\lambda_1} Chl(Z) PAR(\lambda, Z, t) \cdot a^*(\lambda) \phi_{\mu}(\lambda, Z, t) d\lambda dZ dt \quad (3)$$

This has been applied previously in ocean waters (Morel, 1991; Smyth et al., 2005). In the northern North Atlantic the WRM was more accurate than the VGPM for satellite models of primary production (Tilstone et al., 2015). This was primarily because the VGPM has more sensitivity to variations in temperature than the WRM.

3.1.4 Carbon-based models

An example of a carbon-based approach estimates PP in the water column as a function of phytoplankton carbon (C), the growth rate (μ), euphotic zone depth (Z_{eu}) and a parameter related to light adjusted physiology ($f_3(E)$) (Behrenfeld et al., 2005). This can be expressed as follows:

$$PP_{eu} = C \times \mu \times Z_{eu} \times f_3(E) \quad (4)$$

This approach intends to remove dependence on an empirical value for assimilation efficiency, allowing for changes in chlorophyll driven by growth rate, light or biomass (Lee et al., 2015). However, a subsequent study found PP_{eu} derived using this model is often proportional to chlorophyll concentration (Westberry et al., 2008).

3.1.5 Phytoplankton absorption models

The absorption-based model for PP requires input of an optical property (phytoplankton absorption, a_{ph}) rather than a biological parameter (chlorophyll, Chl) (Marra et al., 2007). Kiefer and Mitchell (1983) first described a general model for PP at depth z as follows:

$$PP(z) = \int \varphi(z) \times a_{ph}(z, \lambda) \times E(z, \lambda) d\lambda \quad (5)$$

Where E is light (PAR) at the sea surface, $E(0)$, a_{ph} is the absorption coefficient of phytoplankton pigments and φ is the quantum yield for photosynthesis. Knowledge of the light attenuation coefficient (K) is also required.

Initial results for this approach are promising in ocean waters (e.g. Southern Ocean; Lee et al., 2011). This approach has also been successful in coastal waters (Western English Channel and North Sea), including for size fractionated PP (Barnes et al., 2014). However, at present, applications of this model using satellite derived estimates of a_{ph} are lacking, largely due to the uncertainty surrounding retrieval of a_{ph} from satellite data.

4 Initial retuning and validation

4.1 Historic dataset

A historic dataset of in situ PP was made available for the Venice Lagoon and the Adriatic Sea, 2003-2009 (CNR-ISMAR). This was used to test empirical and VGPM approaches to estimate PP, then forced with MERIS and AASTR satellite parameters to model PP. The results form the foundation for a PP model from Sentinel-3 and are presented below.

4.1.1 Methods

4.1.1.1 *In situ*

Water samples were collected or measured in situ at 6 stations in the Venice Lagoon (n=17) and 4 unique stations in the Adriatic Sea (n=29), between 2003 and 2009 (Figure 1).

Marine PP is most commonly measured by the Carbon-14 (^{14}C) method (Steemann Nielsen, 1952), and was the method used for this historic dataset. Samples were labelled with a known amount of ^{14}C -bicarbonate. After incubation, carbon fixation was quantified by liquid scintillation counting to detect ^{14}C in organic form. Dissolved and particulate organic carbon was quantified after acidification to remove the inorganic fraction. PP analysis was measured using a 6 x 15 chamber photosynthetron (irradiance $0\text{-}2500\ \mu\text{mol m}^{-2}\ \text{s}^{-1}$, temperature $5\text{-}35^\circ\text{C}$).

The Venice Lagoon PP data were simulated in situ incubations in the laboratory for surface samples only, while the Adriatic Sea PP data were depth-integrated samples which were incubated in situ for 1 to 4 hours around noon at 14°C .

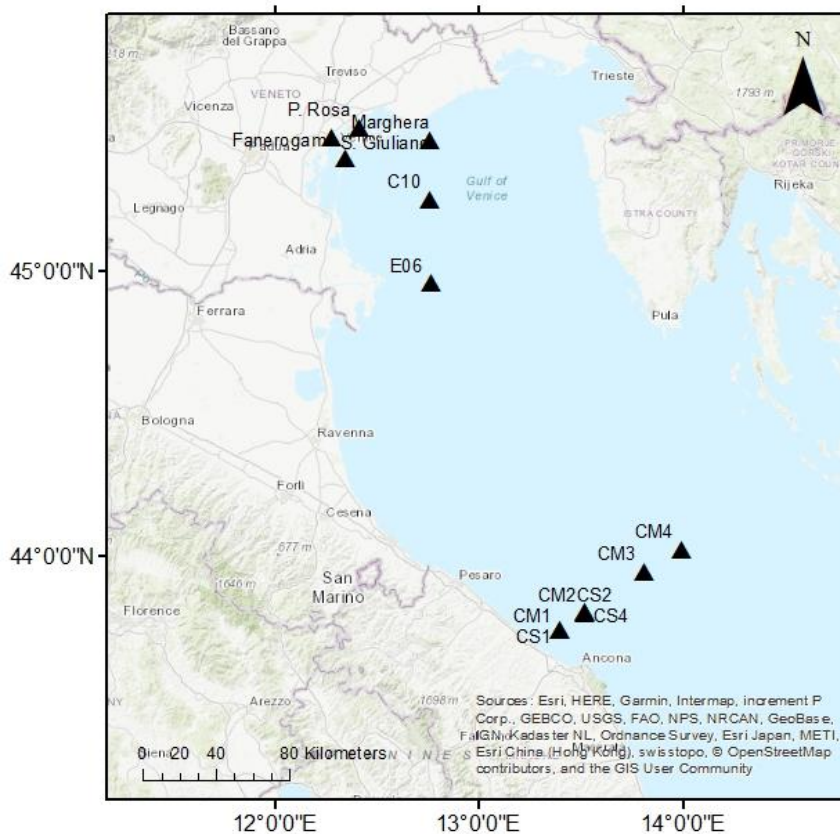


Figure 1. Map of Historic PP measurement stations in the Venice Lagoon and Adriatic Sea.

4.1.1.2 Models

Both empirical and the VGPM were implemented for the historic dataset, as described in Section 3.1.2. These models include variables which were readily available in the historic dataset, while wavelength-resolved and absorption-based models require data that was unavailable.

The empirical model of PP was implemented as in Behrenfeld et al. (1998), according to the following Equation 1.

The VGPM was implemented as in Behrenfeld and Falkowski (1997), according to Equation 2. The parameters for the *in situ* VGPM are defined as follows:

- P_{opt}^B = maximum C fixation rate ($\text{mg C mg Chl-}a^{-1} \text{ h}^{-1}$), modelled as a function of temperature (T),
- E_0 = in situ daily sea surface photosynthetically available radiation (PAR; E m^{-2}), either as daily value or estimated from surface rates ($\text{E m}^{-2} \text{ s}^{-1}$) using D_{irr} ,
- Z_{eu} = euphotic depth (m) calculated from in situ $K_d(\text{PAR})$ profiles (Kirk, 1994) or Secchi depth (Luhtala & Tolvanen, 2018),

- $Chl-a_s$ = surface Chlorophyll-*a* concentration,
- D_{irr} = daily photoperiod, calculated as a function of latitude and day of year using geosphere package in R.

4.1.2 Performance of *in situ* empirical model

4.1.2.1 Retuned empirical model parameters

The empirical model was retuned to the Venice Lagoon and the Adriatic Sea datasets, according to a second order polynomial. The site-specific empirical models were as follows, including a model for surface PP in Venice lagoon (PP_s) and a depth-integrated model for the Adriatic (PP_{eu}). The relationships between PP and Chl-*a* are shown in Figure 2.

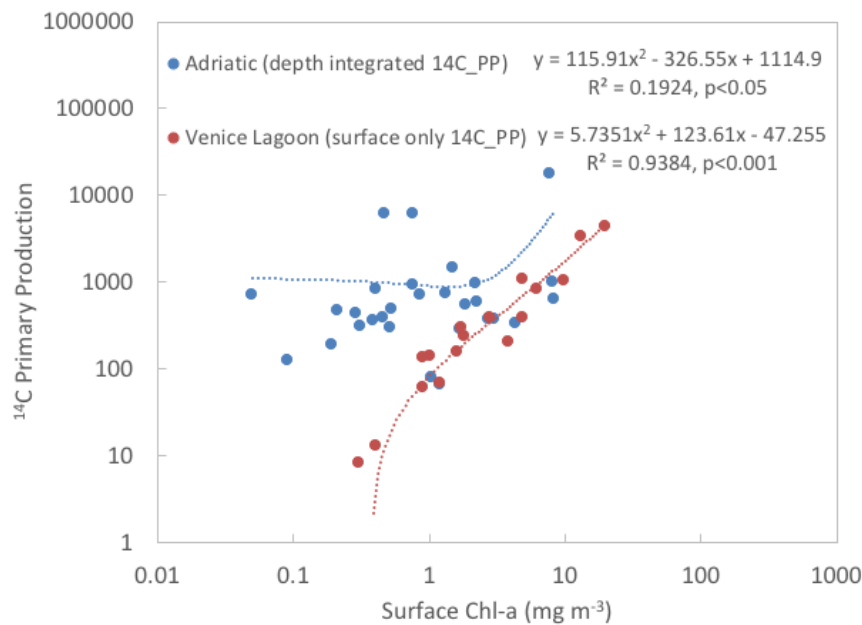


Figure 2. Empirical relationship between PP and Chl-*a* for Venice Lagoon and the Adriatic Sea.

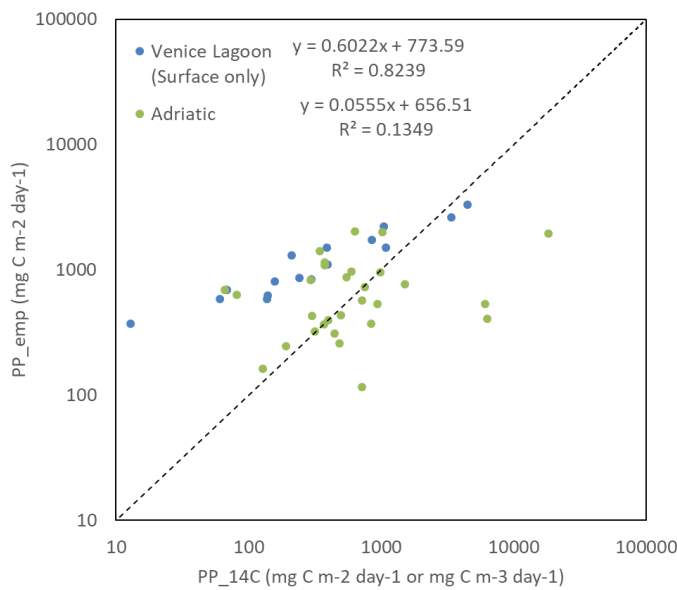
Thus, the site-specific empirical models derived for Venice Lagoon and the Adriatic Sea are as follows:

$$\text{Venice Lagoon: } PP_s = 5.7351 * [Chl - a]^2 + 123.61 * [Chl - a] - 47.255 \quad (6)$$

$$\text{Adriatic Sea: } PP_{eu} = 115.91 * [Chl - a]^2 - 326.55 * [Chl - a] + 1114.9 \quad (7)$$

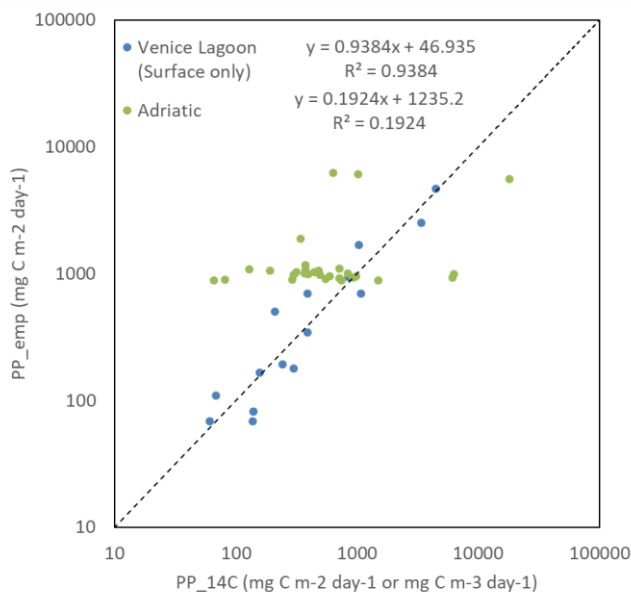
4.1.2.2 Model validation

The results from *in situ* validation of the empirical models are shown in Figure 3 for the Behrenfeld et al. (1998) model. Validation results for the site-specific tuned models are shown in Figure 4. The site-specific model performed better than the Behrenfeld et al. (1998) model for the Venice Lagoon surface PP. However, there was poor performance for the Adriatic using either the Behrenfeld et al (1998) or the site-specific tuned empirical model, indicating this model is likely unsuitable for use in this site.



Error Metric	Value
RMSE_log	0.620
MAE_log	0.476
MAPE	321%
Bias_log	-0.226

Figure 3. *In situ* validation results for empirical model (as in Behrenfeld et al. 1998)



Error Metric	Value
RMSE_log	0.484
MAE_log	0.376
MAPE	183%
Bias_log	-0.189

Figure 4. *In situ* validation results for site-specific empirical models.

4.1.3 Performance of *in situ* VGPM

4.1.3.1 Retuned VGPM parameters

The VGPM was implemented in three ways to test its performance, and these are outlined below.

VGPM

First, the VGPM was implemented as in as in Behrenfeld and Falkowski (1997), modelling P_{opt}^B as a 7th order polynomial function of temperature (T , °C), as follows (note all T for the Venice Lagoon and Adriatic Sea historic dataset ranged from 5-28°C and were therefore modelled):

$$P_{opt}^B = \begin{cases} 1.13 & T < -1.0 \\ 4.00 & T > 28.5 \\ P_{opt}^{B'} & \text{other value for } T \end{cases}$$

where

$$\begin{aligned} P_{opt}^{B'} = & 1.2956 + 2.749 \times 10^{-1}T + 6.17 \times 10^{-2}T^2 \\ & - 2.05 \times 10^{-2}T^3 + 2.462 \times 10^{-3}T^4 - 1.348 \\ & \times 10^{-4}T^5 + 3.4132 \times 10^{-6}T^6 - 3.27 \times 10^{-8}T^7. \end{aligned} \quad (8)$$

mVGPM

In this modified version of the VGPM (mVGPM), P_{opt}^B was modelled using a linear model derived for Loch Leven in the INFORM project as follows:

$$P_{opt}^B = 0.1523T + 0.24 \quad (9)$$

m2VGPM

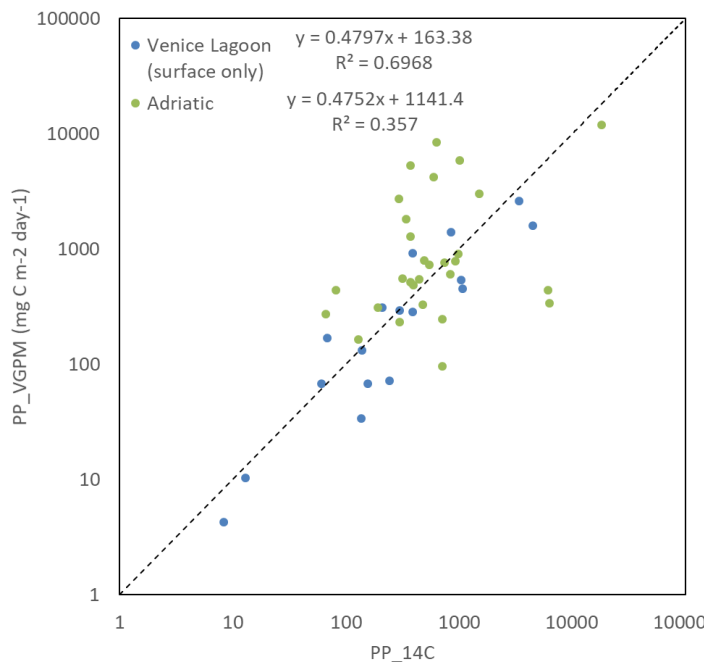
The VGPM was modified a second time (m2VGPM) whereby P_{opt}^B was modelled using the General Lakes 3rd order polynomial, as in INFORM project:

$$P_{opt}^B = 0.00137T^3 - 0.048T^2 + 0.6044T + 0.159 \quad (10)$$

4.1.3.2 Model validation

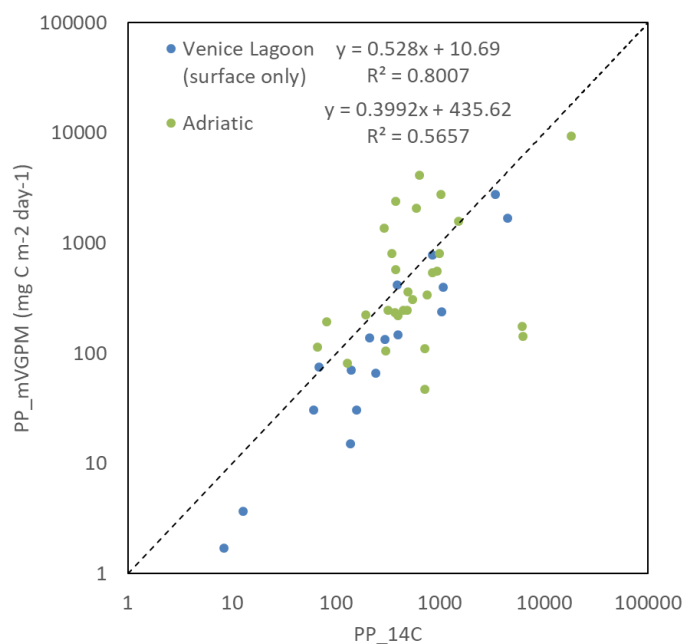
Validation plots of modelled PP as a function of in situ (¹⁴C) PP are shown in Figure 5. The lowest errors are for the m2VGPM (Figure 5c), where P_{opt}^B was modelled as a 3rd order polynomial for General Lakes, indicating this parameterisation of P_{opt}^B also performs best in coastal waters.

(a)



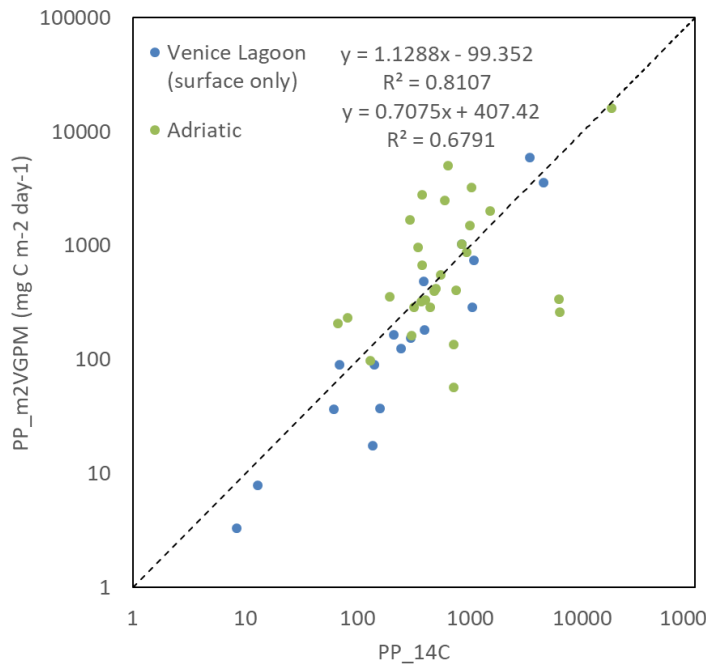
Error Metric	Value
RMSE_log	0.522
MAE_log	0.390
MAPE	168%
Bias_log	-0.0540

(b)



Error Metric	Value
RMSE_log	0.561
MAE_log	0.428
MAPE	89.9%
Bias_log	0.229

(c)



Error Metric	Value
RMSE_log	0.495
MAE_log	0.361
MAPE	100%
Bias_log	0.0763

Figure 5. Validation of (a) VGPM, (b) mVGPM and (c) m2VGPM with in situ data and associated errors.

4.1.4 Performance of satellite model

Level 2 full resolution (L2 FR) MERIS data were acquired from the MERCI website (<https://merisfrs-merci-ds.eo.esa.int>). L2 data are atmospherically corrected with the Case 2 Regional (C2R) algorithm. Cloud, land and coastline pixels were removed using the L2 masks. Matchups with in situ PP data were extracted +/-1 day of the satellite overpass, resulting in 28 matchups for validation.

The site-specific empirical models (Equations 6 and 7) were forced with satellite derived Chl-*a* (Chl-*a*_{sat}) from MERIS. Several empirical, semi-empirical and semi-analytical models were tested, with the best performer applied in the model.

4.1.4.1 Performance of MERIS Chl-*a*

For these data, the best performing Chl-*a* was the standard algal_2 product (Figure 6). The algal_2 product is an Inverse Radiative Transfer Model-Neural Network (IRTM-NN) for Chl-*a*, aCDOM, TSM for Case 1 and 2 waters. However, we note this performed better for the Adriatic than the Venice Lagoon. This product was used for satellite-derived Chl-*a* in both the empirical model and VGPM validation (Sections 4.1.4.2 through 4.1.4.4).

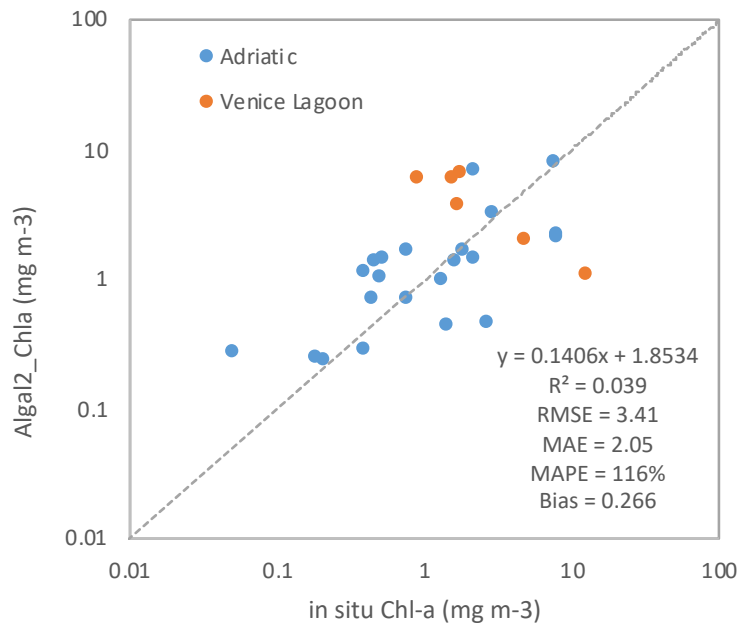


Figure 6. Validation of MERIS L2 algal_2 Chl-a product for Venice Lagoon and the Adriatic Sea

We note that the PP model performance is highly dependent on a good Chl-*a* retrieval. Indeed, a recent sensitivity analysis on PP model input parameters found that Chl-*a* has the greatest effect (Tilstone et al., 2015). Thus, this is a fundamental issue that also needs to be addressed for a Sentinel-3 PP product, and the Chl-*a* and PP validation results will be presented in **D3.8** Validation Report.

Additionally, it is possible that in some coastal areas (e.g. Venice Lagoon) the Chl-*a* retrieval could be impacted by bottom visibility or seagrass presence. For the Sentinel-3 PP product, we will investigate the use of a coastline buffer zone and a shallow water mask (e.g. using a threshold for a modified Normalised Difference Water Index, NDWI) in order to remove pixels affected by bottom influence. A threshold value of NDWI will be used as a mask to remove influence of bottom in shallow waters. The NDWI is a reflectance index used to detect and delineate surface waters or areas of drought, which will be applied for bottom detection from Sentinel-3 OLCI data as follows:

$$NDWI = (\rho_{green} - \rho_{NIR}) / (\rho_{green} + \rho_{NIR}) \quad (11)$$

where ρ_{green} and ρ_{NIR} are the reflectance of green and NIR bands, respectively (McFeeters, 1996). Other studies have applied a modified NDWI using the SWIR rather the NIR band (e.g. Xu, 2006), and this will also be tested. The NDWI ranges from -1 to 1, and generally a threshold of $NDWI > 0$ represents water while non-water or bottom influence is represented by $NDWI \leq 0$. However, previous studies have found that the threshold used should be adjusted to achieve a

more accurate result (Xu, 2006; Ji et al., 2009). Therefore, a suitable NDWI threshold will be determined and applied as a mask to remove bottom influence in shallow waters.

4.1.4.2 Empirical model validation

The validation results for the empirical site-specific models for PP are shown in Figure 7.

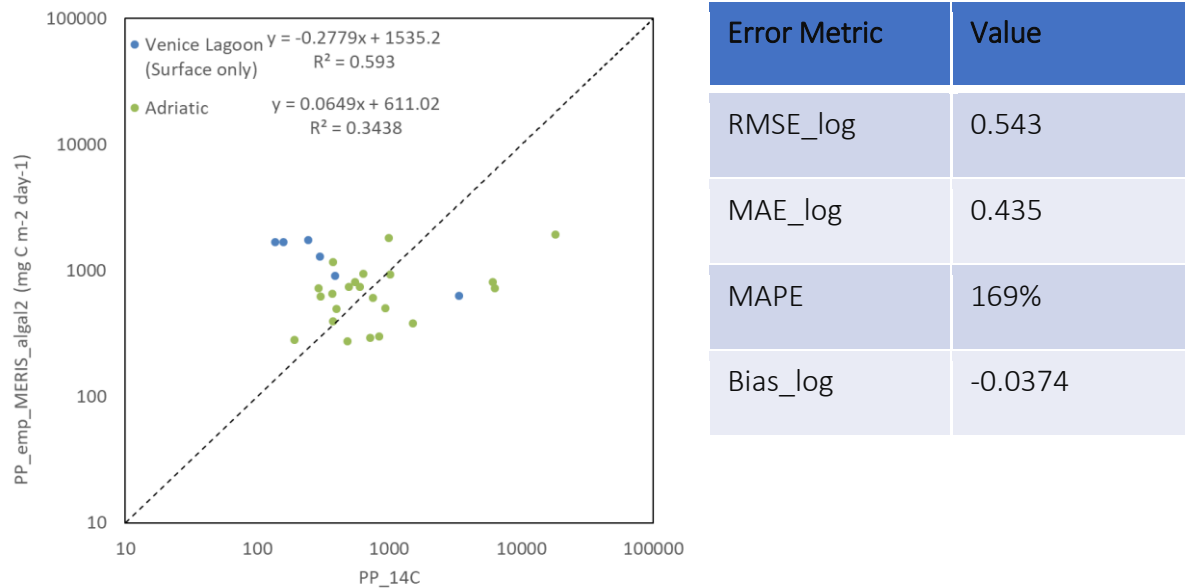


Figure 7. Validation plot and errors for PP derived from MERIS algal_2 Chl-a using site-specific empirical models.

4.1.4.3 m2VGPM model parameterisation

The satellite parameters used as input for the m2VGPM are outlined below, followed by the validation results.

The m2VGPM was implemented as in Equation 2, where the model inputs were sourced as follows:

- **Chl- a_s** (mg m⁻³) = satellite derived Chl-a from the best performing algorithm (MERIS L2 algal_2)
- **Z_{eu}** (m) = derived from MERIS K_d(490) and calibrated with Adriatic or Venice lagoon in situ Z_{eu} from K_d(PAR) or Z_{SD}, respectively.
- **D_{irr}** = daily photoperiod, calculated for MERIS overpass date as a function of latitude and day of year using geosphere package in R
- **E₀** = MERIS L2 daily sea surface PAR (E m⁻²) product

- $P_{opt}^b = m2VGPM$ - parameterised for General Lakes (GL) as in Equation 10, with Level 2 gridded AATSR data acquired to obtain sea surface temperature (SST).

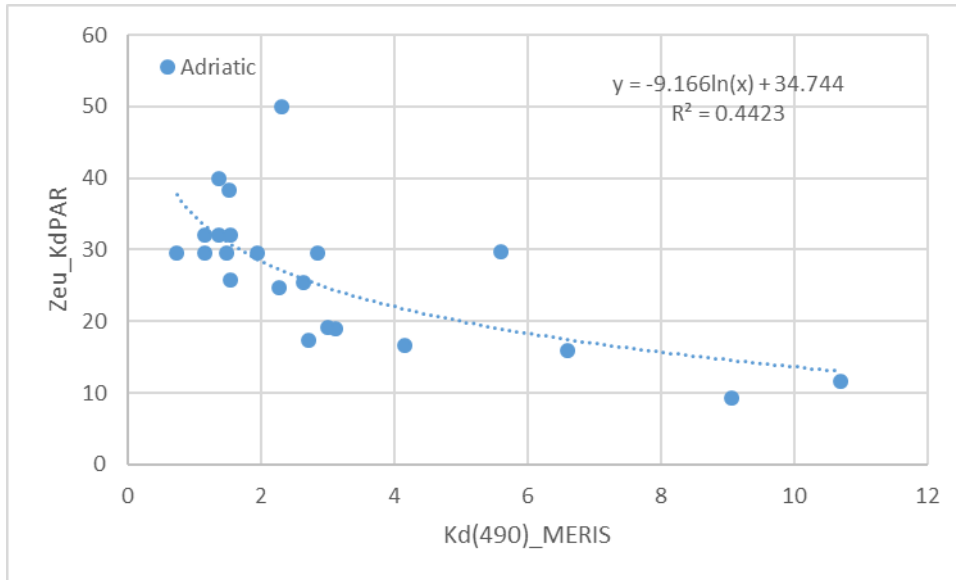
We note that as AATSR data are 1 km spatial resolution, a single nearest pixel extraction resulted in a large decrease in the number matchups due to contamination with land pixels (n=12). All remaining matchups were thus for the Adriatic Sea only.

In order to obtain Z_{eu} , MERIS $K_d(490)$ was first derived from the L2 reflectances as follows:

$$K_d(490) [m^{-1}] = 3.752 \left[\frac{R_{rs}(560)}{R_{rs}(490)} \right]^{1.245} - 0.16 \quad (11)$$

Z_{eu} was then returned using *in situ* estimates of Z_{eu} (in situ Z_{eu} derived from $K_d(PAR)$ and Z_{SD} for the Adriatic and Venice Lagoon, respectively). The calibration plots are shown in Figure 8.

(a)



(b)

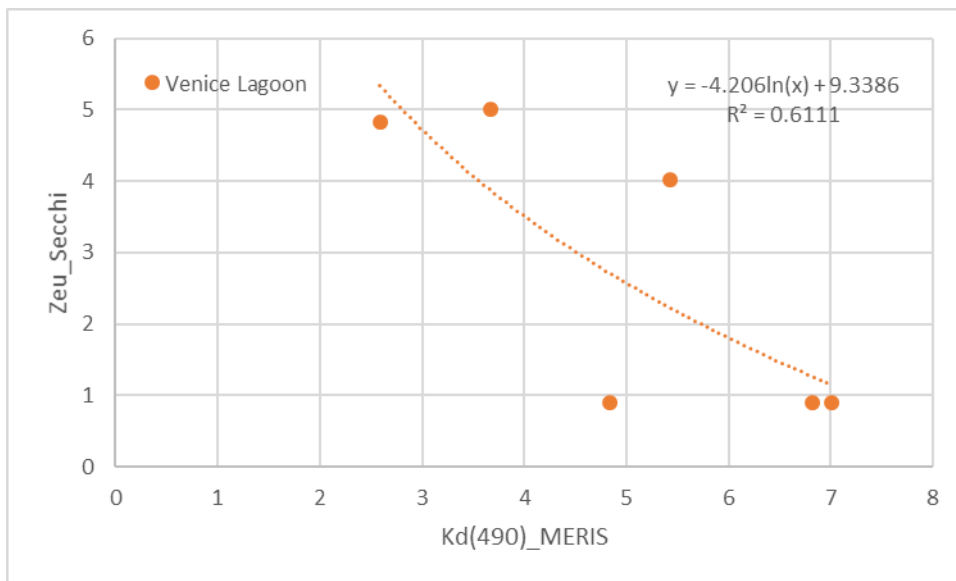


Figure 8. Site specific derived relationship for Zeu as a function of Kd(490) MERIS L2 product in the (a) Adriatic Sea and (b) Venice Lagoon.

Following retuning, the site-specific functions for deriving Z_{eu} from MERIS L2 $K_d(490)$ are as follows:

$$\text{Adriatic: } Z_{eu} \text{ [m]} = -9.66 * \ln(K_d(490)) + 34.744 \quad (12)$$

$$\text{Venice Lagoon: } Z_{eu} \text{ [m]} = -4.206 * \ln(K_d(490)) + 9.3386 \quad (13)$$

4.1.4.4 Model validation

Chlorophyll-*a* (Chl-*a*)

The MERIS algal_2 Chl-*a* product was validated as in the empirical model (see Section 4.1.4.1; Figure 6).

Sea Surface Temperature (SST)

The AATSR SST product performed well and showed a strong relationship with *in situ* temperature (Figure 9).

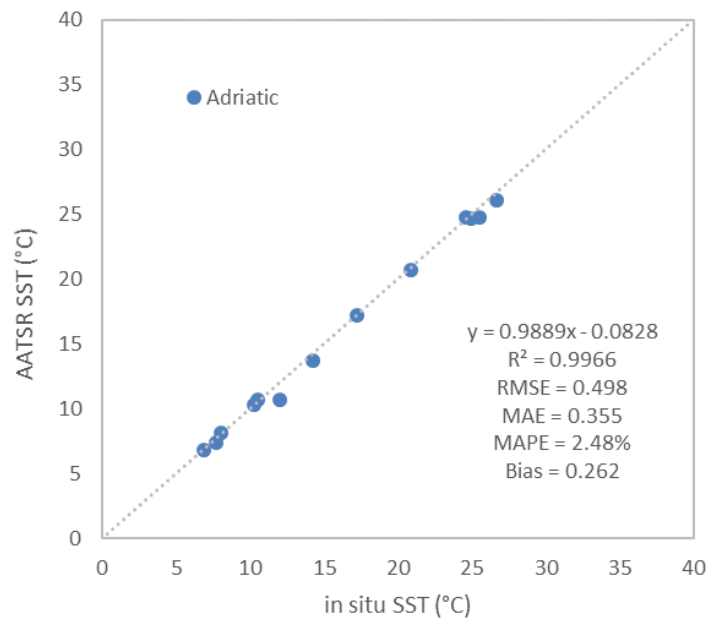


Figure 9. AATSR L2 gridded sea surface temperature (SST) as a function of *in situ* SST (°C).

We do note the limitations of the AATSR product for use in coastal areas, given the large pixel size (1 km). Thus, for the development of the Sentinel-3 PP product, in addition to the Sentinel-2 Sea and Land Surface Temperature Radiometer (SLSTR) SST data, we will also consider the use of the Group for High Resolution Sea surface Temperature (GHRSSST) Level 4 SST data (<https://www.ghrsst.org>). While this is also a 1 km product, the GHRSSST dataset uses multiple satellite as well as moored buoy data sources which provides more opportunity for matchup with *in situ* measurements. Furthermore, the Level 4 product was found to correspond well with *in situ* SST in the Eems Estuary, Netherlands (Water Insight, unpublished data).

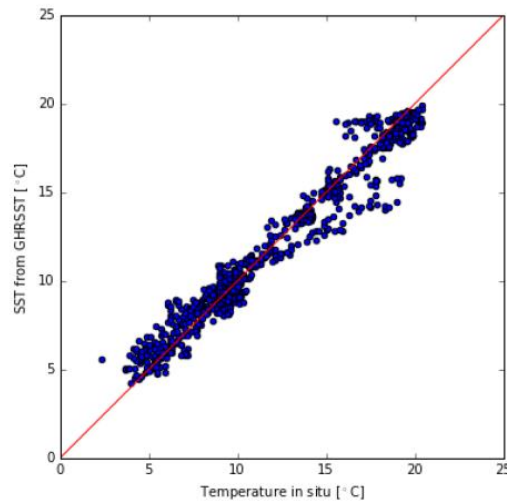


Figure 10. GHRSSST as a function of *in situ* sea surface temperature (°C) for 7 stations in the Eems Estuary, Netherlands (Water Insight, Unpublished data).

Surface irradiance (E_0)

E_0 was the MERIS L2 standard PAR product. Validation for same-day matchups of E_0 is shown in Figure 11, however it is noted this is not particularly good agreement. The error is likely due to the fact that sea surface PAR may change substantially in a short space of time (e.g. from the timing of the satellite overpass to the time of *in situ* measurement), therefore it is not a surprise that there is a poor matchup. For validation in future, surface irradiance measurements will be taken as close to satellite overpass timing as possible.

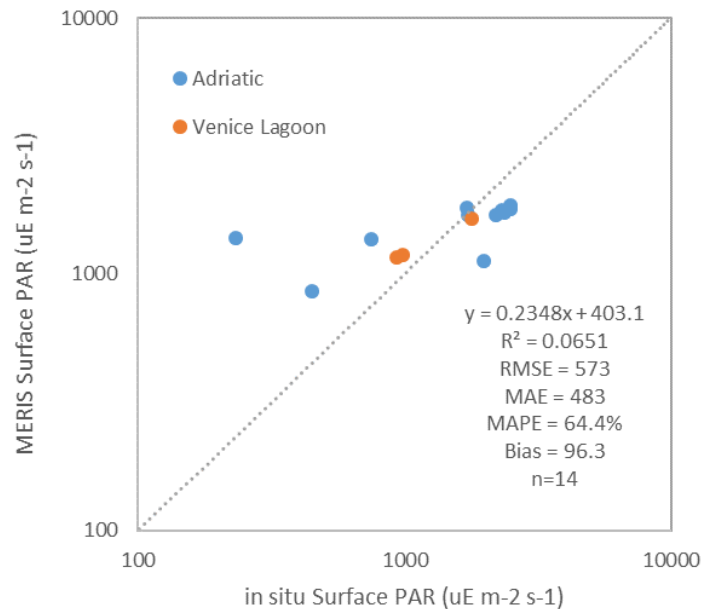


Figure 11 . Validation plot of MERIS L2 surface photosynthetically available radiation (PAR) as a function of *in situ* surface PAR.

Euphotic Depth (Z_{eu})

Z_{eu} derived from MERIS agreed well with that measured in situ at both sites (Figure 12). The euphotic zone was deeper at the Adriatic Sea sites, as compared to the Venice Lagoon, which is as expected.

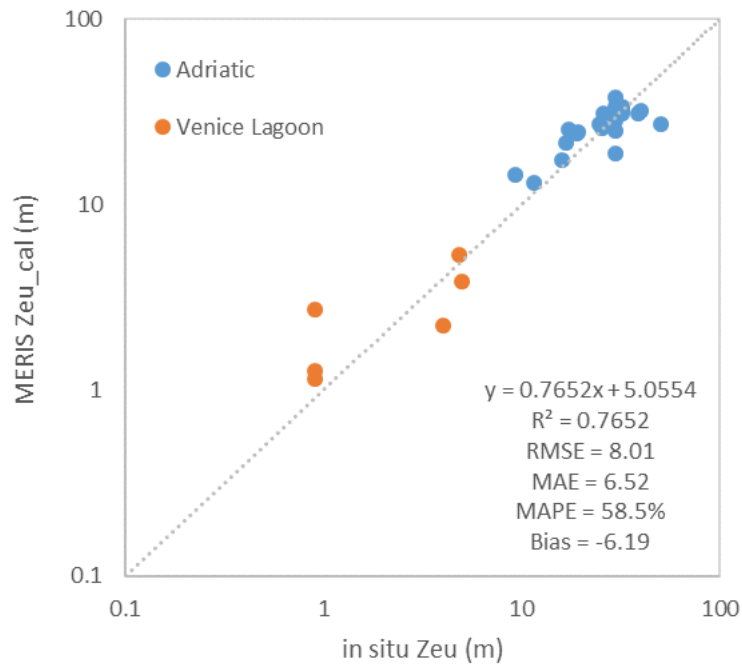
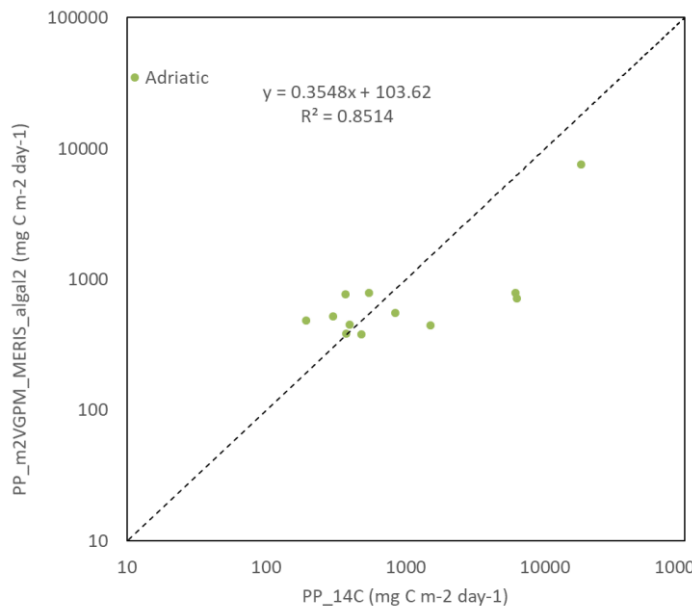


Figure 12. MERIS derived Euphotic depth (Z_{eu}) as a function of in situ Z_{eu} .

Primary Productivity (PP_{eu})

Validation results for m2VGPM applied to MERIS and AATSR data were only possible for the Adriatic Sea dataset, as the AATSR pixel size (1 km) meant the SST product was unviable in the Venice Lagoon due to proximity of land. Satellite derived PP agreed well with in situ ^{14}C PP measurements in the Adriatic, however we note there is a small sample size ($n=12$; Figure 13). An example map of PP for MERIS derived using the m2VGPM is shown in Figure 14.



Error Metric	Value
RMSE_log	0.455
MAE_log	0.350
MAPE	62.8%
Bias_log	0.153

Figure 13. Validation plot and errors for PP_{eu} derived from MERIS and AATSR for the Adriatic Sea.

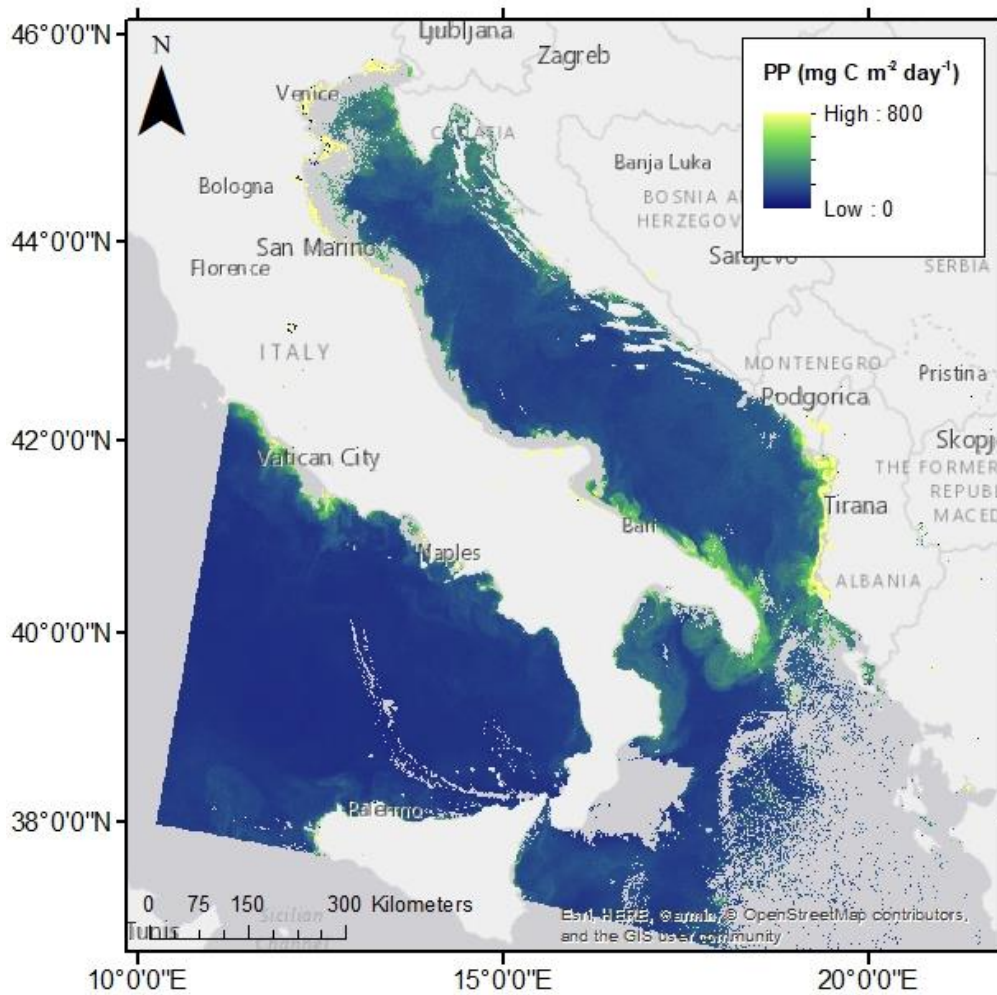


Figure 14. PP derived from MERIS (m2VGPM model; 2005-07-14)

4.2 2018-2019 dataset

During 2018, *in situ* PP measurements were unfortunately not possible. The established method for measuring PP *in situ* requires the use of the radioactive isotope ^{14}C , and a photosynthetron. We were unfortunately unable to gain the necessary permissions to use a radioactive isotope and bring the photosynthetron from the UK (University of Stirling) to the field sites in Italy (CNR-ISMAR) and Vigo (Universidad de Vigo). Therefore, we decided to purchase the Chelsea Act2 instrument in 2018 as an alternative approach, which would avoid the use of radioactivity for PP measurements (Figure 15).

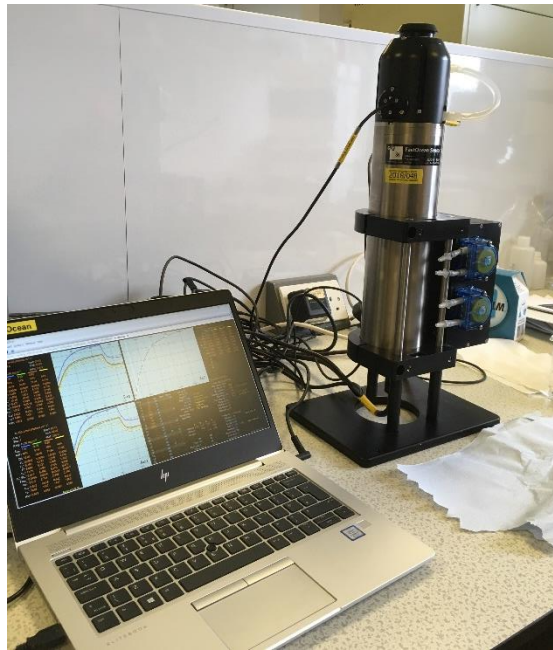


Figure 15. The Chelsea Act2 set up for laboratory based simulated in situ measurements by fast repetition rate fluorometry (FRRf).

In 2018, data were collected at three coastal sites as part of the CoastObs validation campaigns to support development of the PP product (Table 1). Although no measurements were made for PP, samples were collected for Chl-*a* analysis to support validation of the satellite Chl-*a* product also needed for a PP product. Additionally, further campaigns are planned for 2019 to collect Chl-*a* and PP validation data, coincident with Sentinel-3 overpasses, for development of the CoastObs PP product.

Table 1 – Summary of field campaigns completed and planned in support of PP product validation (2018-2019)

Location	Samples collected	Campaign dates
Venice Lagoon and the Adriatic Sea (Italy)	Chl- <i>a</i> Chl- <i>a</i> Chl- <i>a</i> and PP (FRRf)	2-8 May 2018 25-28 June 2018 15-28 July 2019 (planned)
Ria de Vigo (Spain)	Chl- <i>a</i> Chl- <i>a</i> Chl- <i>a</i> and PP (FRRf)	30 May 2018 04-17 July 2018 01-22 June 2019 (planned)
Wadden Sea and the Eastern Scheldt (Netherlands)	Chl- <i>a</i>	Weekly April – October 2018
	Chl- <i>a</i> and PP (FRRf)	11-17 August 2019 (planned)

4.2.1 Methods

4.2.1.1 *In situ*

Samples were collected from the surface and kept cool in the dark for filtration within 24 hours. Water samples were filtered through Whatman GF/F filter papers and stored in cryovials at -80°C prior to analysis.

For analysis of total Chl-*a*, filter paper pigment was extracted in 3 ml of methanol according to the LOV method (Claustre and Ras, 2005). This included freezing at -20°C (minimum 30 min), sonication (10s), freezing again at -20°C (minimum 30 min), then clarification of each sample by syringe filtration. Finally, samples were analysed within 24 hours by High Performance Liquid Chromatography (HPLC). Sample collection and Chl-*a* analysis will be conducted by the same method in 2019.

For the 2019 campaigns, integrated temperature profiles will be measured at each station. The diffuse attenuation coefficient (K_d) will be measured using a LiCOR LI-193-R spherical underwater quantum sensor. SST will be measured using a standard temperature probe. Secchi depth (m) will also be acquired using a standard Secchi disk in order to derive the euphotic depth.

In situ PP will be measured by Fast Repetition Rate fluorometry (FRRf) using the Chelsea Fast Ocean Act2 laboratory system. This method works by quantifying the rate of electron transport through photosystem II (PSII), ETR_{PSII} (Kolber et al., 1998; Oxborough et al., 2012; Robinson et al., 2014). Previous studies have found that ^{14}C measurements are strongly correlated with FRRf estimates of maximum rate of photosynthesis (P_{max}), light utilisation efficiency (α) and minimum saturating irradiance (E_k) (Robinson et al., 2014).

4.2.1.2 *Model*

The m2VGPM will be applied to Sentinel-3 data as for MERIS (Section 4.1.4.3). However, it is likely that some retuning of the model will be required as *in situ* PP will be measured using the FRRf rather than ^{14}C method. These details will be provided in the Validation Report (D3.8), alongside validation results for the Sentinel-3 PP product.

5 Conclusions and future work

The results for a PP model from MERIS are promising and indicate the potential of the VGPM for use in coastal waters of Italy. However, we did experience unforeseen delays in developing this product for Sentinel-3 due to inability to make ^{14}C PP measurements in 2018. Therefore, we purchased the Chelsea Act2 instrument in 2018 as an alternative approach, which avoids the use of radioactivity for PP measurements. The Act2 method has already been trialled at University of Stirling and is prepared for laboratory-based measurements of samples from the 2019 field campaigns. Future work will validate the VGPM in Italy, Spain and Netherlands coastal waters, using measurements of PP from the forthcoming 2019 field campaigns.

This dataset of in situ PP measurements will coincide with Sentinel-3 overpasses. The VGPM can then be forced with Ocean and Land Color Instrument (OLCI) and Sea and Land Surface Temperature Radiometer (SLSTR) or Group for High Resolution Sea Surface Temperature (GHRSSST) data in order to produce a satellite PP product for CoastObs, which will then be validated with the *in situ* PP measurements by FRRf. The validation results for the Sentinel-3 PP product will be presented in **D3.8** (Validation Report).

6 References

- Behrenfeld, M.J., Boss, E., Siegel, D.A. and Shea, D.M. (2005) Carbon-based ocean productivity and phytoplankton physiology from space. *Global Biogeochemical Cycles*, 19(1).
- Behrenfeld, M.J. and Falkowski, P.G. (1997a) A consumer's guide to phytoplankton primary productivity models. *Limnology and Oceanography*, 42(7): 1479-1491.
- Behrenfeld, M.J. and Falkowski, P.G. (1997b) Photosynthetic rates derived from satellite-based chlorophyll concentration. *Limnology and Oceanography*, 42(1): 1-20.
- Behrenfeld, M.J., Prasil, I., Kolber, Z.S., Babin, M., Falkowski, P.G., (1998) Compensatory changes in Photosystem II electron turnover rates protect photosynthesis from photoinhibition. *Photosynthesis Research*, 58(3): 259-268.
- Chassot, E., Bonhommeau, S., Dulvy, N.K., Melin, F., Watson, R., Gascuel, D. and Le Pape, O. (2010) Global marine primary production constrains fisheries catches. *Ecol. Lett.* 13, 495–505.
- Cloern, J.E., Foster, S.Q. and Kleckner, A.E. (2014) Phyto-plankton primary production in the world's estuarine-coastal ecosystem. *Biogeosciences* 11, 2477–2501.
- Eppley, R.W. Temperature and phytoplankton growth in sea. *Fishery Bulletin*, 70(4): 1063-1085.
- Field, C.B., Behrenfeld, M.J., Randerson, J.T., and Falkowski, P. (1998) Primary production of the bio-sphere: integrating terrestrial and oceanic components. *Science*, 281(5374), 237-240.
- Ji, L., Zhang, L. and Wylie, B. (2009) Analysis of dynamic thresholds for the Normalized Difference Water Index. *Photogrammetric Engineering & Remote Sensing*, 75(11): 1307-1317.
- Kolber, Z.S., Prasil, O., Falkowski, P.G. (1998) Measurement of variable chlorophyll fluorescence using fast repetition rate techniques: defining methodology and experimental protocols. *Biochim. Biophys. Acta*, 1367 (1): 88-106.
- Lee, Z., Lance, V.P., Shang, S., Vaillancourt, R., Freeman, S., Lubac, B., Hargreaves, B.R., Castillo, C.D., Miller, R., Twardowski, M., Wei, G., (2011) An assessment of optical properties and primary production derived from remote sensing in the Southern Ocean (SO GasEx). *J. Geophys. Res.* 116. [http://dx.doi.org/10.1029/2010JC006747\(C00F03\)](http://dx.doi.org/10.1029/2010JC006747(C00F03)).
- Lee, Z., Marra, J., Perry, M.J., Kahru, M. (2015) Estimating oceanic primary productivity from ocean color remote sensing: A strategic assessment. *Journal of Marine Systems*, 149: 50-59.
- Marra, J., Trees, C.C., O'Reilly, J.E. (2007) Phytoplankton pigment absorption: a strong predictor of primary productivity in the surface ocean. *Deep-Sea Res.* 1 54, 155–163.

- McFeeters, S.K. (1996) The use of Normalized Difference Water Index (NDWI) in the delineation of open water features, *International Journal of Remote Sensing*, 17(7): 1425–1432.
- Morel, A. (1991) Light and marine photosynthesis—A spectral model with geochemical and climatological implications. *Progress in Oceanography*, 26: 263–306.
- Oxborough, K., Moore, C.M., Suggett, D.J. , Lawson, T. , Chan, H.G. , Geider R.J. (2012) Direct estimation of functional PSII reaction centre concentration and PSII electron flux on a volume basis: a new approach to the analysis of Fast Repetition Rate fluorometry (FRRf) data. *Limnol. Oceanogr. Methods*, 10: 142-154.
- Passow, U. and Carlson, C.A. (2012) The biological pump in a high CO₂ world. *Mar. Ecol. Prog. Ser.* 470, 249-271.
- Robinson, C., Suggett, D.J., Cherukuru, N., Ralph, P.J., Doblin, M.A. (2014) Performance of Fast Repetition Rate fluorometry based estimates of primary productivity in coastal waters. *Journal of Marine Systems*, 139: 299-310.
- Smyth, T.J., Tilstone, G.H. and Groom, S.B. (2005) Integration of radiative transfer into satellite models of ocean primary production. *Journal of Geophysical Research – Oceans*, 110 (C10).
- Steemann Nielsen, E. (1952) The Use of Radioactive Carbon (C¹⁴) for Measuring Organic Production in the Sea. *ICES Journal of Marine Science*, 18(2): 117–140.
- Tilstone, G.H., Smyth, T.J., Gowen, R.J., Martinez-Vicente, V. and Groom, S.B. (2005) Inherent optical properties of the Irish Sea and their effect on satellite primary production algorithms. *Journal of Plankton Research*, 27(11): 1127-1148.
- Tilstone, G.H., Taylor, B.H., Bondeau-Pattisier, D., Powell, T., Groom, S.B., Rees, A.P., and Lucas, M.I. (2015) Comparison of new and primary production models using SeaWiFS data in contrasting hydrographic zones of the northern North Atlantic. *Remote Sensing of Environment*, 156: 473-489.
- Westberry, T., Behrenfeld, M.J., Siegel, D.A. and Boss, E., (2008) Carbon-based primary productivity modeling with vertically resolved photoacclimation. *Global Biogeochemical Cycles*, 22(2).
- Xu, H. (2006) Modification of normalised difference water index (NDWI) to enhance open water features in remotely sensed imagery, *International Journal of Remote Sensing*, 27(14): 3025–3033.